Femtosecond Pump-Probe Measurements of Solvation by Hydrogen-Bonding Interactions

ARTICLE *in* CHEMPHYSCHEM · SEPTEMBER 2004

Impact Factor: 3.42 · DOI: 10.1002/cphc.200301004 · Source: PubMed

4 AUTHORS, INCLUDING:

Ehud Pines
Ben-Gurion University of the Negev
83 PUBLICATIONS **2,684** CITATIONS

SEE PROFILE

Femtosecond Pump-Probe Measurements of Solvation by Hydrogen-Bonding Interactions

Ehud Pines,*[a] Dina Pines,[a] Ying-Zhong Ma,[b] and Graham R. Fleming[b]

An additional ultrafast blue shift in the transient absorption spectra of hydrogen-bonding complexes of a strong photoacid, 8-hydroxypyrene 1,3,6-trisdimethylsulfonamide (HPTA), over the solvation response of the uncomplexed HPTA and also over that of the methoxy derivative of the photoacid (MPTA) in the presence of the hydrogen-bonding base was observed on optical excitation of the photoacid. The additional 55 ± 10 fs solvation response was found to be about 35% and 19% of the total C(t) of HPTA in dichloromethane (DCM) when it was hydrogen-bonded to dimethylsulfoxide (DMSO) and dioxane, respectively, and about 29% of the total C(t) of HPTA in dichloroethane (DCE) when it was hydrogen-bonded to DMSO. We have assigned this additional dynamic spectral shift to a transient change in the hydrogen bond (O–H···O) that links HPTA to the complexing base, after the electronic excitation of the photoacid.

1. Introduction

The study of solute-solvent interactions has long been one of the focal points of solution chemistry.[1–26] Solvation dynamics after excitation of the chromophore to a new electronic state has been the subject of many experimental studies where time-resolved fluorescence Stokes-shift measurements and excited-state transient absorption[1–15] were the important tools as well as absorption line-shape analysis,[16–18] resonance Raman scattering[19–20] and coherent techniques.[21–23] Solute–solvent interactions are mainly due to the dielectric properties of the solvent. Since the range of the Coulomb interaction is large compared to the structure in the radial distribution function of the solvent, such interactions are often termed "nonspecific", implying that no specific chemical bonds are formed or broken between the solvent and the solute. Another common type of solute-solvent interaction results from hydrogen bonding. In this case, hydrogen bonds are formed between specific solute and solvent atoms.[7] Both types of solvation interactions act to reduce the free energy of the solute. In the event of rapid excitation of the chromophore to a new electronic state, the solvent rearranges itself around the solute molecule, so as to re-minimize the free energy of the solute in its newly formed electronic state.

The dynamic aspects of polar solvation have been studied extensively over the past 30 years and have resulted in a detailed description of polar solvation.[1–26] In contrast, relatively few studies on the dynamic aspects of solvation by specific hydrogen-bonding interactions have been carried out.[7–8,27–33] These experiments have been performed on a limited number of hydrogen-bonded complexes. In view of the great variety, high abundance and crucial importance of the hydrogen-bonding interaction to solution chemistry and biochemistry, it is clear that much additional experimental work is needed to comprehend the dynamic aspects of the hydrogen-bonding interactions. In particular, the effect of intermolecular hydrogen-bonding interactions on the electronic states of a solute has been extensively studied in steady-state solution-chemistry.[34–36] A systematic extension of these studies to the time domain is essential for our complete understanding of such processes as solvation dynamics and proton-transfer reactions.[37]

Another domain where understanding the role of hydrogen-bonding interactions is of great importance is in biological environments, which are usually of low polarity. In low polarity environments, intra- and intermolecular hydrogen-bonding interactions rival the energies of nonspecific polar interactions. Indeed, hydrogen-bonding interactions often stabilize and determine the 3D structure of large biological structures such as proteins and DNA, and can play an important role in determining the reactivity of the active site of enzymes.[38]

Herein we report femtosecond time-resolved pump–probe measurements of a novel hydrogen-bonded system in solution, described below. The transient pump-probe data has been treated in terms of the time-dependent absorption correlation function, given in Equation (1):[1]

$$C(t) = \frac{\nu(t) - \nu(\infty)}{\nu(0) - \nu(\infty)} \quad (1)$$

where $\nu(t)$ is the first moment of the excited-state absorption spectrum at time t. In the case of the uncomplexed chromophore $C(t)$ provides comparable information on solvation dynamics to that of time-resolved fluorescence (Stokes-shift) measurements. We have found that the $C(t)$ of the hydrogen-bonded chromophore reveals additional (over polar solvation) dynamics associated with transient hydrogen-bonding interac-

[a] Dr. E. Pines, Dr. D. Pines
Chemistry Department, Ben-Gurion University of the Negev
P.O.B. 653, Beer-Sheva 84105, (Israel)
Fax:(+972) 8-6472-943
E-mail: epines@bgumail.bgu.ac.il

[b] Dr. Y.-Z. Ma, Prof. G. R. Fleming
Department of Chemistry, University of California Berkeley
Lawrence Berkeley National Laboratory, Berkeley, CA 94720–1460 (USA)

 DOI: 10.1002/cphc.200301004

tions taking place following the electronic excitation of the chromophore.

2. General Background

2.1. Identifying Hydrogen-Bonding Interactions Using Steady-State Spectroscopic Measurements

A common way to identify solute–solvent hydrogen-bonding interactions is by using an empirical correlation between a chosen solvent-sensitive property of a solute and some empirical solvent parameters which scale its hydrogen-bonding interactions. Among the most useful empirical correlations is the Kamlet–Taft (K–T) solvent scale. In the K–T approach, any solvent-influenced property of the solute may be correlated using a multiparameter fit, Equation (2)[34–36]

$$P_{s\text{-}s} = P^0_{s\text{-}s} + s\pi^* + a\alpha + b\beta \qquad (2)$$

where $P_{s\text{-}s}$ is the measured solvent-influenced property of the solute, $P^0_{s\text{-}s}$ is the numerical value of the chosen solute property in a reference solvent (ideally, $P^0_{s\text{-}s}$ should have been the numerical value of the solute property in the gas phase), π^* is the normalized solvent polarity scale, α and β are the solvent acidity and the solvent basicity scales respectively, *s*, *a*, and *b* are the specific (empirical) numerical coefficients that characterize the solute.

In this study we have used K–T analysis as a reliable method for identifying the relative importance of the hydrogen-bonding interactions in the overall polar solvation of a chosen probe molecule. This was estimated by correlating the IR and fluorescence spectra of the probe molecule in various solvents according to the K–T procedure,[39] allowing estimates for each solvent–solute system of the relative importance of the hydrogen-bonding interactions out of the total solvent–solute interactions.

2.2. Some General Observations on Hydrogen-Bonded Systems in Solutions

Arguably, the best-characterized hydrogen-bonding interactions are of the form –O–H···O. Several empirical correlations are known for this common type of hydrogen bond.[40–46] These include the correlation between the strength of the hydrogen bond and its length. The stronger the hydrogen-bonding interaction, the shorter the hydrogen-bond length. Typical hydrogen-bond lengths vary between about 2 Å for very weak hydrogen bonds to about 1.2 Å for very strong ones, with typical bond energies lying between 1 and 25 kcal mol^{-1}.[40–46] A second important empirical correlation is between the IR absorption peak of the O–H stretching mode (typically, between 2500 and 3800 cm^{-1}) and the strength of the O–H···O hydrogen-bonding interactions.[40–44] The stronger the interaction, the more the IR absorption is shifted towards lower frequencies. This correlation originated with Badger and Bauer's observation that the shift in the A–H stretching mode tends to correlate with the enthalpy required to break the hydrogen bond.[45,46] The down shift in the O–H stretching frequency correlates with the lengthening of the O–H covalent bond as a result of the hydrogen-bonding interaction.

Finally, there are empirical correlations between the strength of the hydrogen-bonding interactions and the acidity and basicity strength of the hydrogen-bond donor (pK_a) and hydrogen-bond acceptor (pK_b).[39,47] For a given hydrogen-bond donor (the acid) the strength of the hydrogen bond tends to increase with an increase in the β value of the hydrogen-bond acceptor (the base). A similar situation occurs for hydrogen-bond acceptors. In these cases, the hydrogen-bond strength increases with the α value of the proton donor.[48]

2.3. Choice of a Suitable Hydrogen-Bond (Donor) Probe

A very useful class of hydrogen-bond donors is hydroxy-aromatic photoacids.[49–50] The acidity of the hydroxy group of these molecules is greatly enhanced in the electronic excited state, thus making them excellent hydrogen-bond donors in the excited state.

Phenol, the simplest of the hydroxy-aromatic photoacids has a $pK_a = 9.9$ in the ground state and a $pK_a^* = 4.3$ in the excited state. Phenol forms strong hydrogen bonds in the ground state, having one of the highest known hydrogen-bond donor coefficients, $a = 1.61$. A very desirable property of phenol derivatives is their ability to form strong 1:1 hydrogen bonds with various weak bases in nonpolar media.[51–52] This specific single hydrogen-bond interaction of the O–H group has been proven to have a marked effect on the spectral features of phenols and naphthols.[53] In fact, this property of the hydrogen-bonding interaction of phenol derivatives was one of the methods used to establish the K–T basicity scale, β. It was also found that excited hydroxypyrene derivatives form one strong hydrogen bond in protic solvents, the O–H···O bond, so these photoacids are only able to donate a hydrogen bond to the solvent, but do not tend to accept one in return.[47]

Herein we have used a derivative of hydroxypyrene, 8-hydroxypyrene 1,3,6-trisdimethylsulfonamide, HPTA, Figure 1 (a). In aqueous solutions HPTA is a weak acid ($pK_a = 5.6$). In the excited-state HPTA becomes a very strong photoacid ($pK^*_a = -0.8$), resulting in fast proton dissociation in aqueous solutions, $k_d = 18$ ps^{-1}. We have correlated the fluorescence Stokes shift of HPTA in various solvents using the K–T procedure.[47] We have found out that for HPTA, up to 50% of the total spectral shift in the fluorescence spectrum of the photoacid may be due to the O–H···O hydrogen-bonding interaction between HPTA and the solvent.

2.4. Choice of Solvent and Proton Acceptor

The following considerations were taken when choosing solutions of dimethylsulfoxide (DMSO) and dioxane in dichloromethane (DCM) and 1,2-dichloroethane (DCE) as the hydrogen-bonding media. DCM and DCE are both polar aprotic solvents with high π^* values (about 0.8) and negligible or small α and β values.[48] Thus the main solvation of HPTA in pure DCM and DCE is through "nonspecific" polar solvation processes with no

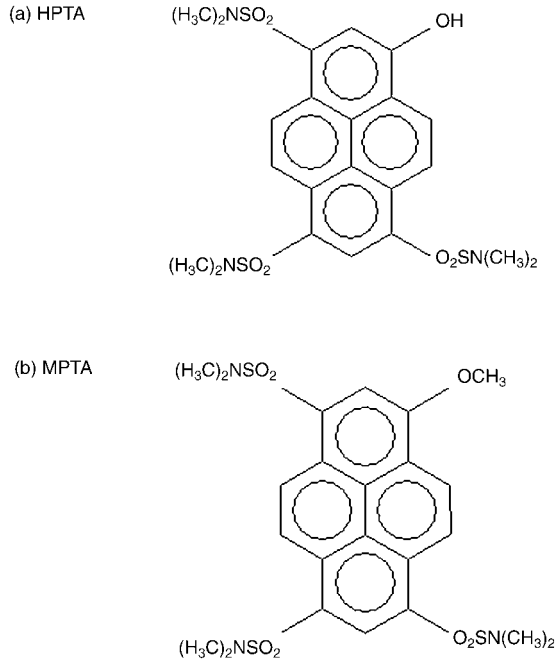

Figure 1. *Structures of HPTA and MPTA.*

significant hydrogen-bond formation. The high π^* value of the solvents is also important for dissolving the relatively polar HPTA molecule in its monomeric form (see additional details in the experimental section). At the same time, DCM and DCE are polar enough so to support strong hydrogen bonding of HPTA to DMSO and dioxane in the form of ground state hydrogen-bonding complexes. Both DMSO and dioxane are aprotic, unassociating solvents which are known to form strong 1:1 complexes with phenol derivatives.[31,32] In the case of HPTA, a O–H···O hydrogen bond is formed in the electronic ground state, whose existence is easily detected by IR absorption (Figure 2) and UV absorption spectroscopy (Figures 3 and 4). The latter method also allowed the quantitative analysis of the hydrogen-bonding equilibrium constant, Figure 5. Furthermore

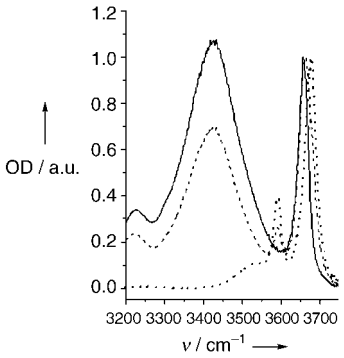

Figure 2. *IR absorption spectra of HPTA in pure DCM (••••), in the presence of 10^{-2} M DMSO (-----) and 2×10^{-2} M DMSO (——). The uncomplexed and complexed IR absorptions of the O–H stretching appear at 3670 and 3420 cm^{-1}, respectively. The absorption peak at 3590 cm^{-1} is from HPTA dimers present due to the large concentration of HPTA needed for the IR absorption experiment (10^{-2} M).*

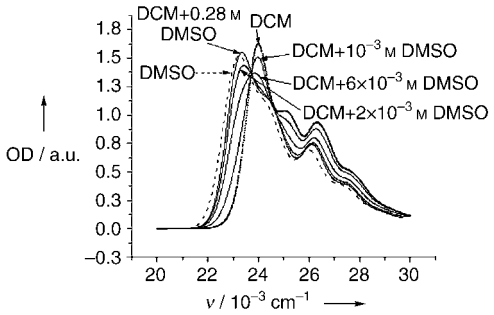

Figure 3. *UV/Vis absorption spectra of 5×10^{-4} M HPTA in various solvents.*

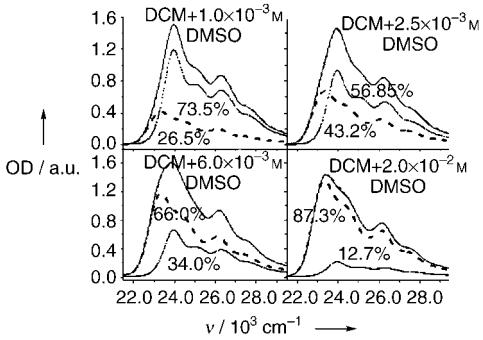

Figure 4. *UV/Vis absorption spectra of 5×10^{-4} M HPTA in solutions of DCM containing various concentrations of DMSO (——), fitted by the linear combination of the fully complexed HPTA taken at 0.28 M DMSO (-----) and the uncomplexed HPTA taken in pure DCM (••••). The population-weighted fits are shown as dashed and dotted lines. The measured and fitted spectra are practically identical.*

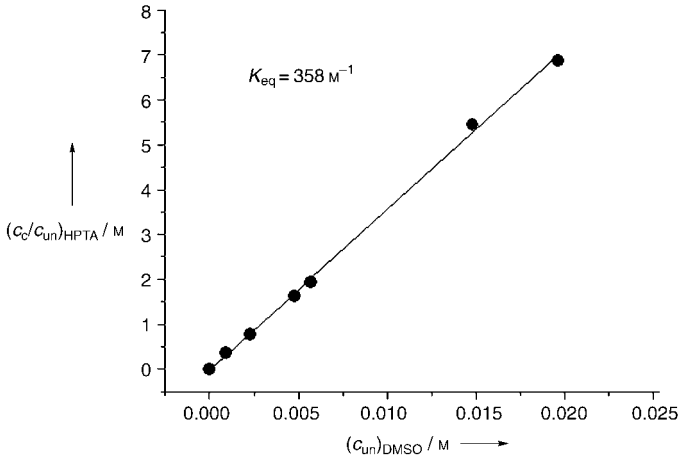

Figure 5. *Ratio of complexed-to-uncomplexed populations HPTA versus the DMSO concentration taken from the spectral fit as shown in Figure 4. The slope of the line is equal to the complexation constant of the hydrogen-bonding complex between HPTA and DMSO in DCM.*

we have found it possible to prepare, in the ground state, large fractions of the photoacid in the hydrogen-bonding form using small amounts of the complexing bases such that the dielectric properties of the solvent environment were not significantly altered by the presence of the base (see below).

2.5. Separation of the Specific and Nonspecific Solvent Effect Using Kamlet–Taft Solvent Empirical Parameters

According to the K–T analysis of the solvent effect, the total fluorescence Stokes shift due to a solvent environment is a linear combination of its hydrogen-bonding interactions (α, β) and its nonspecific polar interactions [π^*; Equation (2)]. Using the K–T idea of the orthogonality of the π^* and β interactions, we have effectively created a DMSO-like environment for HPTA solvation by mixing a nonpolar solvent (DCM or DCE), which has a similar π^* value to that of DMSO (0.8 compared to 1.0 for DMSO), with very small amounts of DMSO. Since in the pure DMSO, HPTA forms only one strong –O–H···O bond, the combined effect of the DCM/DCE-DMSO mixtures in conditions where all HPTA molecules were hydrogen bonded to DMSO was expected to be almost identical with the effect of solvating HPTA in pure DMSO. This was indeed the case as shown in Figure 4. The observed saturation of the solvation energies (hydrogen-bonding interactions (α and β) and nonspecific polar interactions (π^*), at about 5×10^{-2} M concentration of DMSO ensured that the major effect of the added DMSO was through specific interactions with HPTA and not because of nonspecific polar interactions.

3. Method for Separating Transient Hydrogen-Bonding Solvation from Nonspecific Solvation Dynamics

The sub-picosecond polar solvation dynamics of pure DCM and DCE solvents is similar to the sub-picosecond polar solvation dynamics observed in solutions of pure DMSO and dioxane. In all pure solvents the fastest solvation response is in the 150–200 fs time range: DCM, $\tau_1 = 144$ fs (52%); dioxane, 177 fs (46%); DMSO, 214 fs (50%);[7] and DCE, 200 fs (20%)[54] (molecular dynamics calculation). The value in brackets is the relative amplitude of the fastest "inertial" solvation response in the total solvation response.

Applying the K–T analysis for DMSO ($\beta = 0.76$) and for dioxane ($\beta = 0.37$)[27] both in DCM/DCE solutions [Eq. (2)] about 35% and 20% of the total transient solvation response following the electronic excitation of HPTA in DCM/DCE-DMSO and dioxane/DCM solutions respectively is due to the –O–H···O hydrogen-bond interaction in the excited state of HPTA. To separate the pure solvent solvation response and the hydrogen-bonding interaction response following the optical excitation of the photoacid, we have reconstructed the C(t) of HPTA in the pure DCM/DCE solvents and in the same solvents in the presence of small amounts of DMSO and dioxane. The additional (over the pure solvent) component observed in the presence of the complexing oxygen-bases was attributed to the time-response of the hydrogen-bonding complex of the photoacid. As an additional control to the pure solvent control, we have measured the solvation dynamics of the methoxy analogue of the photoacid where no hydrogen-bonding interaction is expected to occur in presence of identical concentration of DMSO, the complexing base, see further discussion below.

4. Control Measurements on the Methoxy Derivative of the Photoacid (MPTA)

Substituting the acidic hydrogen of the OH group with a methyl group effectively diminishes the hydrogen-bond interaction of HPTA (Figure 1b). The absorption spectrum of 8-methoxypyrene 1,3,6-trisdimethylsulfonamide, MPTA, is red-shifted compared to the absorption spectra of uncomplexed HPTA by 339 cm^{-1} and is blue-shifted by only 287 cm^{-1} compared to the fully complexed HPTA (Figure 6). All spectroscopic data

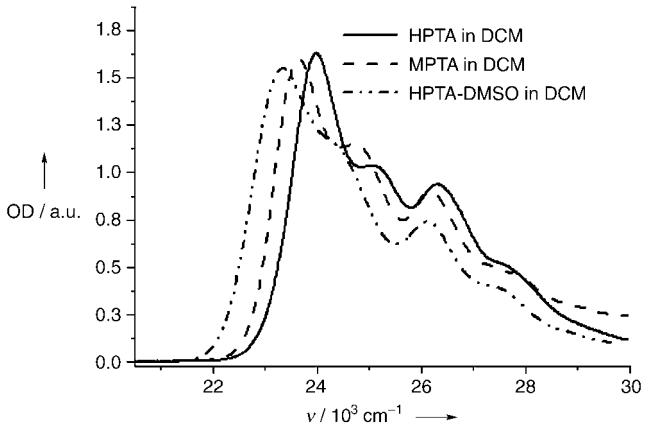

Figure 6. *Comparison of absorption spectra of HPTA, MPTA, and HPTA-DMSO hydrogen-bonding complex in DCM.*

refer to DCM/DMSO solutions. In DCM/dioxane solutions the differences in the spectral shifts are even smaller but not as well-resolved as the shifts in DCM/DMSO solutions due to the much smaller complexation constant HPTA with dioxane. The vibronic structure of the absorption spectra is little changed between HPTA, MPTA, and complexed HPTA in DCM/DMSO solutions (Figure 6). This makes MPTA an excellent control for the HPTA experiments. Together with the neat solvent control it clearly represents the situation where no hydrogen-bonding interactions affect the solvation dynamics of HPTA. In addition, the difference between the excitation energy and the 0-0 energy of MPTS and complexed HPTA is very similar, so MPTS is also a good control for any intramolecular process potentially occurring due to the excess excitation energy put into the HPTA complexes.

5. Results

5.1. Steady-State Studies of HPTA–DMSO in DCM Solutions

Figure 3 shows the absorption spectra of HPTA in DCM solutions with increasing amounts of DMSO. Also included in Figure 3 is the absorption spectrum in pure DMSO. The spectrum shifts 11 nm from 417 nm in pure DCM to 428 nm in 1:50 (0.28 M) DMSO. Adding more DMSO did not noticeably change the absorption spectrum up to almost pure-solvent concentrations. In pure DMSO the spectrum shifts further by 2 nm to 430 nm and becomes a little broader. This is the result of DCE/

DCM being less polar than the pure DMSO solvent. Two clear isosbestic points are observed at 406 nm and 422 nm in all absorption spectra except in that measured in pure DMSO. This shows that the absorption spectrum of HPTA is made of two populations and is the weighted combination of the absorption of the uncomplexed and complexed HPTA. To demonstrate this point further, all absorption spectra of HPTA in DCM of up to 0.28 M concentration of DMSO were fully reconstructed with no additional fitting parameters by combining the uncomplexed with the fully complexed absorption spectra of HPTA (taken in solutions of 0.28 M DMSO in DCM) with relative weights determined by the complexation constant. Figure 4 shows four representative reconstructions of the HPTA absorption spectrum superimposed on the actual measured spectrum of HPTA in DCM/DMSO solutions. The actual and reconstructed spectra are practically indistinguishable from each other.

The relative weights of the uncomplexed and complexed HPTA as a function of DMSO concentration from 10^{-3} M up to 0.28 M DMSO confirms a 1:1 complexation process between HPTA and DMSO with a complexation constant $K_{HB} = 358 \pm 20\ M^{-1}$, (Figure 5). The molar ratio between the photoacid and the complexing base was varied in the above concentration range between 2:1 to 560:1 DMSO:HPTA and the molar ratio between the solvent and DMSO was varied from 10000:1 to 50:1 with no apparent change in the position or the structure of the absorption spectrum of neither the complexed nor the uncomplexed HPTA. This evidently shows that the excess DMSO, which is not complexed with the photoacid, has little or no effect on the transient absorption spectrum of the photoacid. Presumably, this is because of the much greater excess of the solvent which effectively separates between the uncomplexed DMSO and both the uncomplexed and the 1:1 complexed HPTA. The value of complexation constant found for DMSO is similar to the value reported for *p*-fluorophenol-DMSO 1:1 complexes in CCl_4 ($K_{HB} = 346 \pm 8\ M^{-1}$) measured by IR spectroscopy and calorimetry by Arnett et al.[52] Similar measurements on the hydrogen-bonding complexes between DMSO and phenol in the same solvent resulted in a smaller complexation constant, $K_{HB} = 202 \pm 2\ M^{-1}$.[52] This exemplifies the importance of the complexing acid in determining the magnitude of the complexation constant, its value presumably correlated in this case to the difference in the ground-state acidity between the two acids. For HPTA in DCM/dioxane solutions a much smaller complexation constant $K_{HB} = 40 \pm 5\ M^{-1}$ was found by reconstructing the HPTA absorption and fluorescence spectra as described above for DMSO. This K_{HB} value is comparable with the value $K_{HB} = 17.7\ M^{-1}$ found for fluorophenol–THF complexes in CCl_4.[52]

Figure 7 shows the practically nonexistent effect of adding 10^{-2} M DMSO to a 5×10^{-4} M DCE solution of MPTA in which the acidic hydrogen atom of HTPA is replaced by a methyl group and no hydrogen-bonding interactions with DMSO occur. Figure 8(a) shows the shift in the fluorescence spectrum of HPTA as a result of adding 9×10^{-3} M DMSO to a DCM solution (this was a typical concentration in our studies at which about 80% of the HPTA was complexed). The relative shift in the fluorescence spectrum is more than twice as large as the shift in the absorption spectrum. In contrast, no shift was observed in the fluorescence of MPTA in the same solution [Figure 8(b)]. This observation again points to the null effect of the uncomplexed DMSO on the optical spectra of the chromophore when they are both dissolved in large excess of DCM and DCE solvents but not directly interacting.

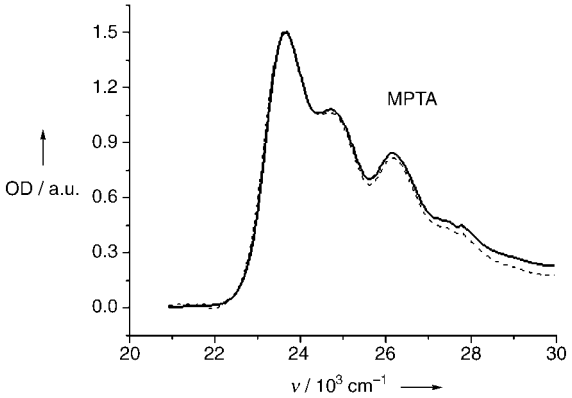

Figure 7. *UV/Vis absorption spectra of MPTA in pure DCM (——) and in solution of DCM in presence of 10^{-2} M DMSO (----).*

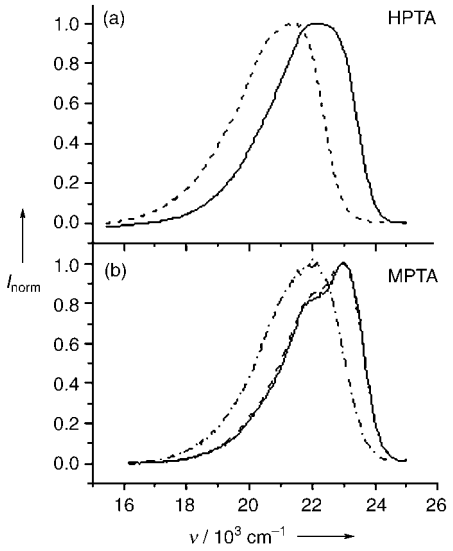

Figure 8. *(a) Fluorescence spectra of HPTA in pure DCE (——) and in DCE in the presence of 10^{-2} M DMSO (----). (b) Fluorescence spectra of MPTA: in pure DCE (——), and in DCE in the presence of 2×10^{-2} M DMSO (----). The red-shifted fluorescence spectrum of MPTA in pure DMSO is shown for comparison (–•–•).*

5.2. Time-Resolved Studies of HPTA–DMSO and HPTA/Dioxane in DCM and DCE Solutions

The transient absorption kinetics of HPTA in the pure solvents and in the hydrogen-bonded complexes were measured at fixed wavelengths. The individual curves were independently best-fitted to a sum of four exponential components using an iterative deconvolution scheme. Figure 9(a) compares the transient absorption kinetics of HPTA in pure DCM at 590 nm and in a 9×10^{-3} M solution of DMSO in DCM at 570 nm. The two

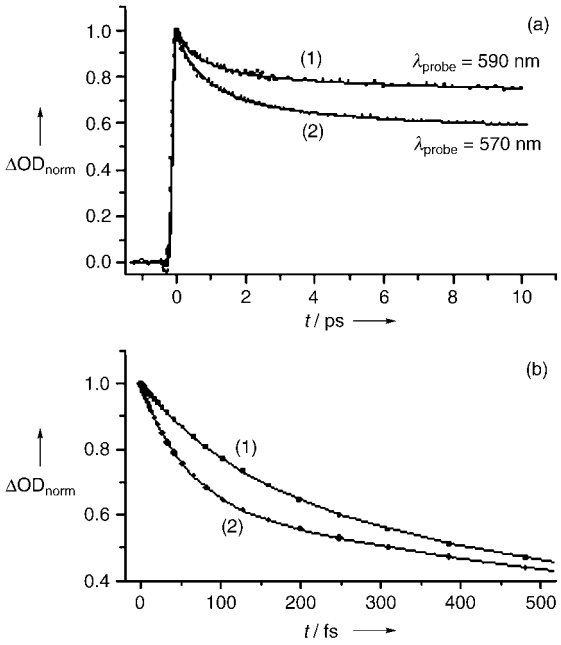

Figure 9. *(a) Normalized transient absorption decays for HPTA in pure DCM measured at 590 nm (1) and in DCM in the presence of 9×10^{-3} M DMSO measured at 570 nm (2). The experimental data are shown by symbols and the corresponding fits are shown by solid lines. (b) The same transient absorption data as shown in (a) after subtracting the long (3.5 ns) excited-state decay component and renormalizing the data.*

wavelengths are at the red side of the absorption spectrum of HPTA and have been so chosen to compensate for the spectral shift in the ground state absorption spectra between the DMSO complexes and uncomplexed HPTA. Comparison at identical wavelengths resulted in an even larger change between the uncomplexed and complexed HPTA transient absorption kinetics (not shown). The parameters of the deconvolution fitting are summarized in Table 1. Evidently, the transient absorption kinetics of HPTA in the presence of DMSO contains additional faster decay components and the total amplitude of the transient spectral shift is much larger than the corresponding transient absorption data for HPTA in pure DCM. Figure 9(b) shows the time-fits of the same transient absorption data after subtracting the long-lifetime decay component (3.5 ns) of the excited state and after normalizing the data. These single-wavelength measurements contain "raw" experimental data and only serve to indicate the presence of additional ultrafast dynamics in the HPTA–DMSO data, (Table 1), but should not be treated quantitatively. The equivalent control experiment is shown in Figure 10. Figure 10 compares the transient absorption of MPTA in pure DCM and in presence of 9×10^{-3} M DMSO. The comparison is made for several representative absorption wavelengths. The two sets of measurements have been found to be identical, within experimental resolution, in the spectral range: 620–470 nm. The identical temporal behavior, within our sub-100 fs time resolution, of MPTA in the pure solvent and in the presence of DMSO agrees with the negligible spectral change observed in the steady-state measurement, Figure 7. The temporal behavior of the single wavelength transient absorption spectra of MPTS has also been found to be identical with the temporal behavior of HPTA in the pure solvent when a small (time-independent) spectral shift between the two absorption spectra was assumed (Figure 11). The 10-nm spectral shift is similar to the one found between their respective steady-state absorption spectra (Figure 3). This suggests that both uncomplexed HPTA and MPTA undergo similar polar solvation dynamics in the pure DCM and DCE solvents.

Table 1. *Best-fitting parameters for the transient absorption kinetics of HPTA in pure DCM and in a 9×10^{-3} M solution of DMSO in DCM, probed at 590 and 570 nm, respectively.*

	DCM 590 nm	DCM + DMSO (80%)[a] 570 nm
A_1 [%]	7	19
τ_1 [fs]	149	56
A_2 [%]	15	21
τ_2 [ps]	0.67	0.78
A_3 [%]	9	13
τ_3 [ps]	4.27	4.17
A_4 [%]	69	47
τ_4 [ns]	3.50	3.50

[a] Percentage of hydrogen-bonding complex.

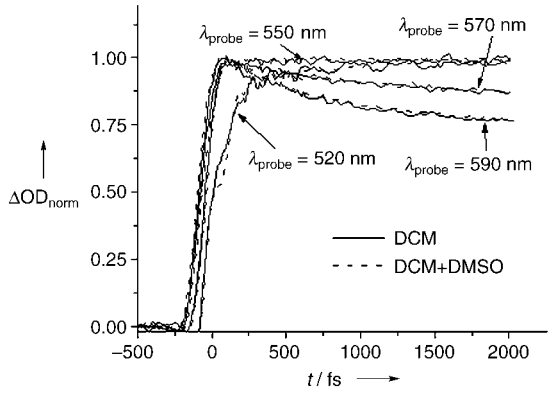

Figure 10. *Comparison of the transient absorption of MPTA in pure DCM and in the presence of 9×10^{-3} M DMSO taken following excitation at 400 nm (shown for different probe wavelengths).*

We have reconstructed from the single-wavelength measurements such as shown in Figure 9 the transient absorption spectrum of excited HPTA. The reconstructed transient absorption spectrum of HPTA (Figure 12) is influenced by stimulated emission from the S_1-S_0 transition. The absorption and gain bands of the S_1 state of HPTA are well separated at the zero-time and move towards each other due to solvent relaxation (Figure 13); the gain band is red-shifting while the absorption band is blue-shifting. As a result, the overlap between the two bands increases with time, so the area of the absorption spectrum appears to decrease with time. We have, thus, calculated the C(t) function from the red side of the S_1–S_n absorption band (620–515 nm), which is about 60% of the total absorption band, outside the region of overlap with the S_1–S_0 gain

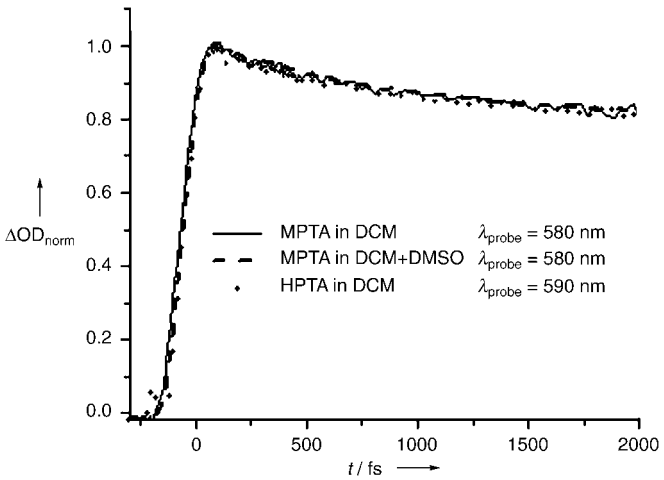

Figure 11. *Comparison of the transient absorption data of HPTA and MPTA in pure DCM and in the presence of 9×10^{-3} M DMSO taken following excitation at 400 nm and shown for different probe wavelengths.*

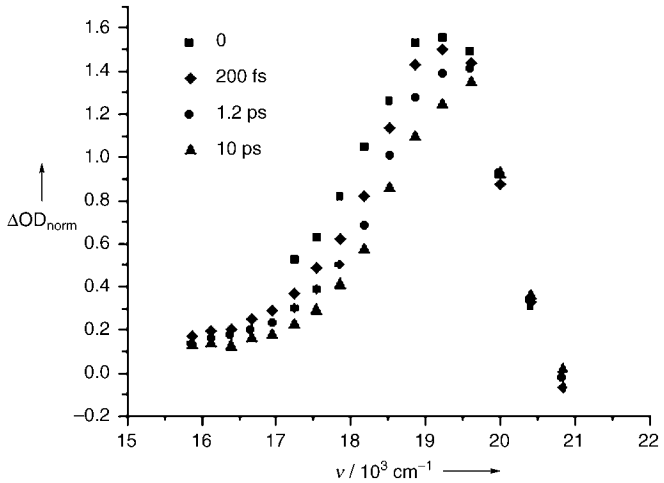

Figure 12. *Transient absorption spectra of HPTA in DCM in the presence of 9×10^{-3} M DMSO taken following excitation at 400 nm.*

band. We were not able to directly measure the full gain band (below 470 nm) due to technical limitations of the experimental set up, hence we could not have used the data of the gain band independently for C(*t*) calculation. The dynamics of the transient gain band (Figure 13) were simulated using the data taken in the range of 620–470 nm. When taking into account the influence of the stimulated emission (gain) band, the area (oscillator strength) of S_1–S_n transition was found to be constant (Figure 13). This implies the absence of an internal-conversion transition to a singlet state having a different oscillator strength as was suggested to occur on a slower time scale (2 ps) for some other hydroxypyrene photoacids.[56]

Figure 14 shows the calculated solvation function, C(*t*), for HPTA in the pure DCM solutions and in presence of 9×10^{-3} M DMSO or 10^{-1} M dioxane, respectively. Figure 15 shows the C(*t*) for HPTA in pure DCE and in the presence of 9×10^{-3} M DMSO.

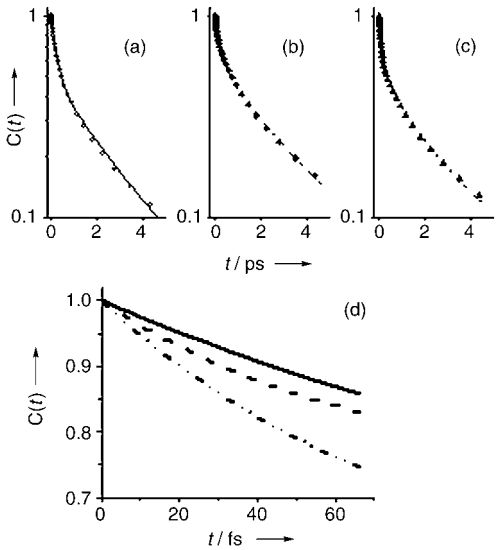

Figure 14. *Logarithmic (a,b,c) and linear (d) plots of calculated C(t) of 5×10^{-4} M HPTA in pure DCM (a), in the presence of 0.1 M dioxane (b), and in presence of 9×10^{-3} M DMSO (c). Parameters of the fits are shown in Table 2.*

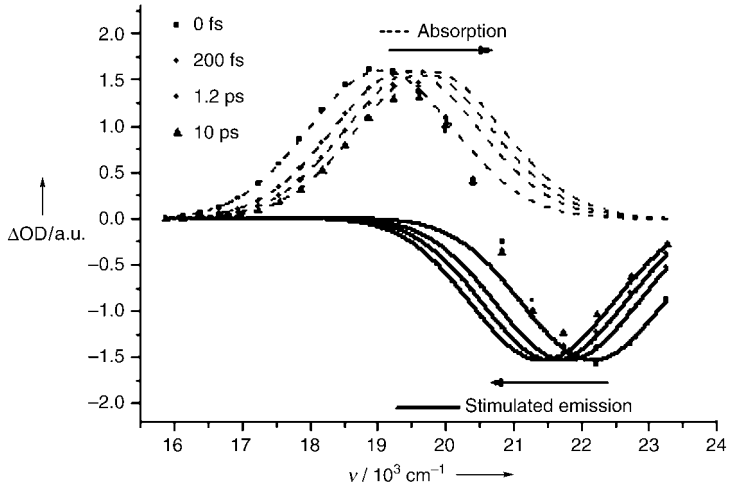

Figure 13. *Reconstruction of the spectra shown in Figure 12 with the time-zero absorption and gain bands moving toward each other due to solvent relaxation.*

In both cases the C(*t*) obtained for HPTA in presence of DMSO or dioxane is seen to be faster than the corresponding C(*t*) observed in the pure solvents.

The C(*t*) functions obtained for the pure solvent and in the presence of DMSO or dioxane were calculated by using Equation (1), where ν_A was given by the first moment of the red part of the transient spectra, and were subsequently fitted using multiexponential global analysis over the full usable part of the single-wavelength data set (pure solvent and in presence of the complexing base). The solvation dynamics in the pure solvents were fitted by sum of two exponentials convoluted with the instrument response function. The overall solvation response upon the addition of DMSO or dioxane was fitted by a sum of three decaying exponential components, two of which were chosen to be identical (both temporally

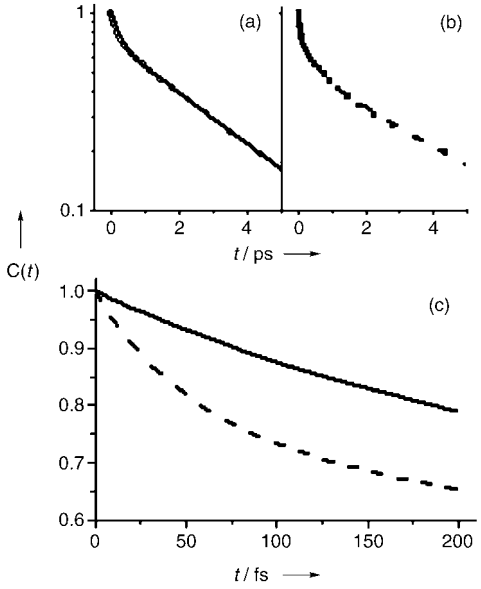

Figure 15. *Logarithmic (a,b) and linear (c) plots of calculated C(t) of 5×10^{-4} M HPTA in pure DCE (a) and in presence of 9×10^{-3} M DMSO (b). Parameters of the fits are shown in Table 2.*

and in terms of relative amplitudes) to those obtained in the fits of the solvation dynamics in the pure solvents. The third (additional) decaying exponent was assigned to the hydrogen-bonding complex. The parameters obtained from the global fits of the data taken at 80% complexation (see experimental section) and in pure solvents are summarized in Table 2. The amplitudes after normalization of the sub-100 fs component to 100% complexation are also shown. We have also relaxed the global fits and carried out individual fits of the calculated C(*t*) by best-fitting the data with three decaying exponents. The fastest decaying components in the absorption spectra of HPTA in pure DCM and DCE solvents were found to be 180 and 220 fs, respectively. The corresponding best-fit parameters found by the global analysis of both the pure solvent relaxation dynamics in DCM/DCE and the solvation dynamics in presence of the hydrogen-bonding bases were somewhat slower, 260 and 360 fs for DCM and DCE, respectively. We have thus estimated the uncertainty in the determination of the fastest pure-solvent relaxation component (τ_2) to be about $\pm$70 fs. The fastest decaying component in DCM–DMSO, DCM–dioxane, and DCE–DMSO was 65 fs (34%), 57 fs (19%) and 54 fs (31%), respectively. The corresponding parameters found in the global fits of the data were 56 fs (35%), 60 fs (19%) and 42 fs (29%), all values falling within 5–12 fs of the freely determined parameters. We have estimated the uncertainty in determining the additional (over the pure solvent solvation dynamics) sub-100 fs component (τ_1) to be about $\pm$ 10 fs (see Table 2).

6. Discussion

Over the last several years, a number of groups have reported on the temporal response of hydrogen bonds to several types of perturbations.[21–23,27–33,57–73] Elsaesser, Nibbering, and co-workers[27–32] have conducted a series of time-resolved IR absorption measurements on the hydrogen-bonding interactions of coumarin 102 (C-102). A very similar dye coumarin 153 (C-153) has been widely used in polar solvation studies. In these hydrogen-bonding studies the C-102 molecule was found to act as a base in solution, accepting a hydrogen bond at the C=O site of the coumarin backbone.[31–32] Upon ultrafast electronic excitation the C=O···H bond was cleaved within 200 fs, which indicates that the excited coumarin molecule becomes a weaker base. Elssaeser, Nibbering, and co-workers have concluded the hydrogen-bond breakage is most probably not immediate and that hydrogen-bond dynamics are likely to occur below their time resolution (170 fs) following the electronic excitation of the hydrogen-bond acceptor. They have also concluded that it is likely that the dynamics of the hydrogen bond affect the electronic transition akin to solvation dynamics, but were reluctant to explore this observation further because in their experiment the complexing acid was breaking away from the complex and so had ample time, within their time resolution, to react nonspecifically with the chromophore. A conceptually similar experiment was done recently by Palit et al.[33] on ground-state hydrogen-bonding complexes between coumarin 102 and amine bases. The hydrogen bond between C-102 and aniline has been found to break upon optical excitation of C-102 within a time resolution of 250 fs.

Although the evidence for the hydrogen-bonding interaction is clear, the IR measurements do not provide a clear picture of how much this specific hydrogen-bonding interaction influences the results obtained using C-153 as a fluorescence (optical) probe for the nonspecific polar (di-

Table 2. *Parameters for the multiexponential fit of C_A(t).*

	DCM	DCM + DMSO 80%[a]	DCM + DMSO 100%[b]	DCM + dioxane 80%[a]	DCM + dioxane 100%[b]	DCE	DCE + DMSO 80%[a]	DCE + DMSO 100%[b]
A_1 [%]	–	28	35	15	19	–	23	29
τ_1 [fs][c]	–	56	56	60	60	–	42	42
A_2 [%]	40	29	26	33	32	34	26	24
τ_2 [ps][d]			0.26				0.36	
A_3 [%]	60	43	39	52	49	66	51	47
τ_3 [ps]			2.3				3.5	

[a] Percentage of hydrogen-bonding complex. [b] Amplitudes renormalized with A_1 corrected to 100% complexation. [c] The error bars in τ_1 values are $\pm$10 fs. [d] The uncertainty in τ_2 values is $\pm$70 fs.

electric) solvation response of large variety of solvents. In fact, Horng et al.[7] have argued that the effect of hydrogen bonding is small compared to several other uncertainties contributing to the overall spread found in their experimental data. Their argument is certainly reasonable in most solvents because of the large dipole moment of C-153 in the excited state, and the fact that significant hydrogen-bonding interactions only exist in protic solvents. Another factor contributing to mitigating the effect of the hydrogen-bonding interaction on C-153 is that it exists only in the ground state. However, as already observed by Horng et al.,[7] alcoholic solvents, which are excellent hydrogen-bond donors, tend to group together and deviate from their expected pure dielectric response when judged by their transient effect on the C-153 fluorescence spectra. Indeed, inspection of the reported data implies a small dependence of the solvation of C-153 on α, the solvent acidity parameter, in alcohols in addition to the expected dependence on π^*.

Finally, there are recent evidences for sub-150 fs proton-transfer reactions in bimolecular acid-base pairs directly complexed by hydrogen-bonding interactions. The neutralization reaction between a photoacid (HPTS), similar to HPTA, and a base in water triggered after optical excitation, was studied recently by femtosecond vibrational spectroscopy by Rini et al.[74] In hydrogen-bonded acid-base complexes, formed at 1–4 M concentration of the base, the proton transfer proceeds extremely rapidly, within temporal resolution of 150 fs. Another observation of ultrafast bimolecular proton-transfer dynamics within hydrogen-bonding complexes of H_3O^+ and NH_3^+ was made recently by Li and Farrar[64] in cross-beams experiments. The proton transfer occurred within the lifetime of the hydrogen-bonding complex of about 100 fs. These observations also imply even faster ultrafast dynamics of pre-existing hydrogen bonds in the acid–base complex which pave the way for, and facilitate, the proton-transfer reaction.

Herein, we have attempted a different approach when trying to resolve the ultrafast nature of the hydrogen-bonding interaction. We have chosen a probe molecule (photoacid) and relatively nonpolar solvent media where the hydrogen-bonding interaction has a substantial influence on the solvation of the photoacid in the excited state with no subsequent proton transfer reaction. Unlike the coumarin probes, up to 50% of the total solvent effect on the fluorescence spectra of these photoacids may be due to hydrogen-bonding interactions. Even more important is the fact that the hydrogen bond becomes stronger in the excited state of photoacids so there is much less chance for a complexing base to dissociate upon electronic excitation and react nonspecifically with the photoacid. In fact, the hydrogen-bonding complex is likely to become tighter in the excited state of the photoacid, see a detailed discussion below.

Two questions are at the core of our investigation: what is the nature of the dynamic changes occurring at the hydrogen bond following the optical excitation of the photoacid; and what dynamic aspects of the hydrogen-bonding complex immersed in a polar solvent control these changes. Gas phase measurements done on similar photoacids which were hydrogen-bonded to various base molecules have shown the same behavior patterns observed in solution, namely upon the optical excitation of the photoacid the existing (ground-state) hydrogen bond becomes stronger and the average heavy-atom separation in the hydrogen bond becomes shorter. Humphrey and Pratt[65–66] concluded that the hydrogen bond between 1-naphthol and the NH_3 moiety contracts by 0.14 Å after the electronic excitation of 1-naphthol. Leutwyler and co-workers[67–69] conducted several comprehensive studies on the spectroscopy of hydrogen-bonding complexes of photoacids. In all systems studied, they observed the strengthening of the hydrogen bond after electronic excitation. In addition, the stretch frequency of the hydrogen bond has increased and the heavy-atom separation in the hydrogen bond has decreased. The magnitude of the changes was found to depend on the nature of the photoacid, and were typically 3–10% greater than the corresponding values in the ground state. For the 1-naphthol-NH_3 hydrogen-bonding complex, six intermolecular vibration modes were identified and found to be affected by the electronic excitation of the photoacids. These were the stretch vibration of the hydrogen bond, two in-plane wag vibrations, two out-of-plane rocking motions and the ammonia torsion motion. In their 2001 paper, Henseler et al.[68] concluded that "the observed increase of the stretch frequency in the S_1 state reflects a higher curvature due to a strengthening of the hydrogen bond after electronic excitation" and that "the hydrogen-bond strength and the changes in curvature and well depth upon electronic excitation are correlated". Lahmani et al.[70] have studied the electronic and vibrational spectra of jet-cooled hydrogen-bonding complexes of o-cyanophenol. The o-cyanophenol is a strong photoacid which is enhanced by the presence of the cyano group at the ortho position of the phenolic ring. Similar inductive effect appears to be the reason for the much-increased acidity and photoacidity of HPTA as compared to the acidity and photoacidity of hydroxypyrene ($pK_a = 5.6$ and 8.7; $pK^*_a = 4.3$ and -0.8 for HPTA and hydroxypyrene, respectively). An increase of about 10% in the intermolecular vibrational stretch frequencies at about 200 cm^{-1} was found upon the optical excitation of the o-cyanophenol when complexed with several oxygen-bases. Lahmani et al.[70] have observed that "this result indicates a tightening of the structures in the excited state". It is thus reasonable to conclude that as a general role, the geometrical features of gas-phase hydrogen-bonding complexes between a photoacid and a base are expected to dynamically change upon the electronic excitation of the photoacid and the induced increase in its proton acidity. In solution, geometrical changes in the hydrogen-bonding complex may be stabilized by the presence of a polar solvent and thus might be enhanced compared to the gas phase. Zundel and co-workers[75–76] have found linear correlations between the stretch vibration frequency of the hydrogen bond and the acidity constant of several families of ground-state acids complexed to the same base. For substituted phenols complexed with trimethylamine in DCM, the stretch vibration increased from about 165 cm^{-1} to about 280 cm^{-1} when the pK_a of the substituted phenol decreased (so the acidity increased) by only three pK_a units, from about 10.3 to about 7.3. The trend was reversed when the acidity of

the acid was increased further, indicating the transfer of the proton from the substituted-phenol acid to the *N*-oxide base. Another important observation made by Zundel was that when the centers of gravity of the phenols are far from the hydrogen-bonding axis, the stretch vibration was almost entirely determined by the force constants (which in turn were largely dependent on the acidity of the acid) and not by the mass of the binding partners. All these observations suggest that hydrogen-bonding complexes of strong photoacids in solutions may be potentially very sensitive to a change in the acidity of the photoacid upon optical excitation. These changes are likely to result in transient shifts in the energies of the electronic transitions of the photoacid akin to changes caused by transient polar-solvation dynamics.

From Figures 14 and 15, as well as from Table 2, it is clear that the hydrogen-bonding interactions significantly affect the overall spectral evolution of HPTA following the electronic excitation of the photoacid. The calculated C(*t*) curves for the HPTA–DMSO and HPTA–dioxane complexes show that hydrogen-bonding interaction contributes 35% and 20% of the total C(*t*) of HPTA–DMSO in DCM and HPTA–dioxane in DCM, respectively. In addition, this contribution was found to be about 29% of the total C(*t*) of HPTA in dichloroethane (DCE) when it was hydrogen bonded to DMSO. The above amplitudes are comparable to the increase in the spectral shifts due to the hydrogen-bonding interactions found in steady-state spectroscopy using K–T analysis [Eq. (2)]. The time scale of the additional solvation response is ultrafast, sub-100 fs, and perhaps as fast as 50 fs. This lifetime is still much slower than the ground-state vibrational stretching period of the O–H bond at about 3400 cm^{-1}, $\tau(OH) < 10$ fs but is shorter than the period of the stretch vibration of the OH···O hydrogen bond, which is typically between 120 cm^{-1} and 250 cm^{-1}. This translates to a vibrational period in the range of 120 fs $< \tau$ (O···O) < 250 fs. However, it is unlikely that the actual hydrogen-bond dynamics will be purely along the heavy-atom axis, so the stretch vibration may be coupled to off-axis or out-of-plane intermolecular modes which are higher in energy and usually lie in the 250–400 cm^{-1} energy region. In addition, the intermolecular rearrangement within the hydrogen-bonding complex of the excited photoacid is clearly a relaxation phenomenon and follows the change in the intramolecular charge distribution of the photoacid in the excited state. As a result of the intramolecular potential change, the heavy-atom separation in the hydrogen-bond decreases and the intermolecular interaction between the complexing base and the photoacid increases. Such changes can also potentially lead to proton transfer between the photoacid and the base when a full charge separation is energetically stabilized by the combined effect of the large proton-affinity of the base and the presence of nearby polar solvent molecules. We thus suggest that proton-transfer reactions follow the hydrogen-bond (heavy-atoms) dynamics between the acid and base. Interestingly, this was concluded theoretically by Guallar et al.[71] in their molecular dynamics simulations of excited-state double-proton transfer in 7-azaindole hydrogen-bonding dimers. Guallar et al.[71] have found that the double proton transfer is likely to be sequential in this system and that the first proton transfers after an initial nuclear relaxation process which mainly involves the symmetric stretch motion of the two hydrogen bonds connecting the dimer molecules. The heavy-atom configurational-relaxation was calculated to be sub-100 fs. These predictions were in full agreement with the combined experimental and theoretical study of the same system made by Zewail and co-workers.[61] Finally, since intermolecular proton-transfer reactions following electronic excitation of the photoacid may be as fast as sub-150 fs it is consistent to suggest, as our present study implies, that hydrogen-bonding configurational-relaxation under the action of an external potential may be as fast as sub-100 fs. This is indeed the time scale recently emerging in various theoretical and experimental studies of hydrogen-bond dynamics in water where subgroups of the hydrogen-bonding complexes are now thought to relax in time scales as fast as 30 fs.[77–78] In particular, Fecko et al.[72] have recently concluded that changes in the molecular field brought about by intermolecular dynamics act on the proton and are the causes of the observed ultrafast hydrogen-bond dynamics, of which the initial response to the external perturbation was measured to be sub-100 fs.

One may attempt to visualize the changes in the hydrogen-bond geometry by schematically considering the changes along the heavy-atom axis connecting the acid and base molecules through the hydrogen-bonding interaction. Although the actual changes involve many degrees of freedom, the one along the heavy-atom axis is special as it defines the existence of the hydrogen bond as well as defining the reaction coordinate for proton transfer. In contrast to the effect of electronic excitation on the hydrogen-bond length which is formed by the photoacid (getting shorter), the increased acidity of phenol-like photoacids in the excited state is expected to lengthen the O–H covalent bond. Thus, the dynamics due to the transient hydrogen-bonding interaction of a phenol-like photoacid may be schematically viewed by two alternative pictorial perspectives; one showing the transient response of the O–H covalent bond (Figure 16) and the other showing the par-

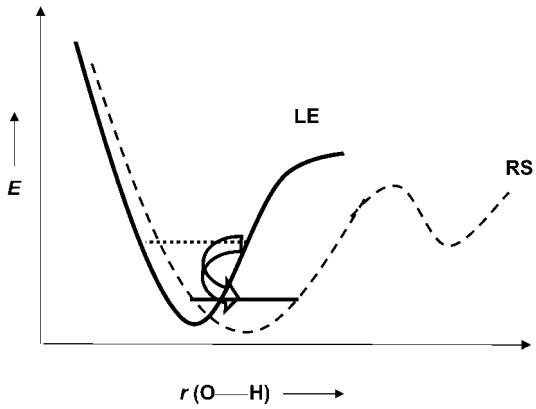

Figure 16. *Schematic response of the O–H covalent-bond in the O–H···O hydrogen bond complex of a phenol-type photoacid after the optical excitation of the photoacid. LE is the local excited state with the O–H bond length and zero-energy projected from the ground state of the photoacid. RS is the relaxed state of the hydrogen bond in the electronic excited state of the hydrogen-bonded photoacid, which has a (slightly) longer O–H bond length and a smaller zero-energy value.*

allel response along the O···O hydrogen-bond coordinate (Figure 17). The latter perspective of the effect of electronic excitation on the hydrogen-bonding interaction originates from Pimentel.[40]

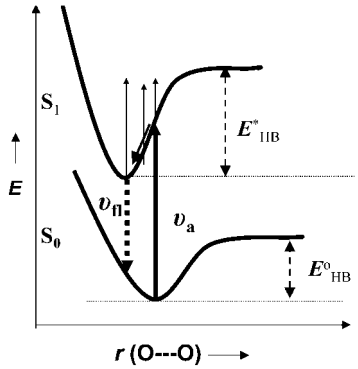

Figure 17. Schematic response of the OH···O hydrogen bond in the hydrogen-bonding complex of phenol-like photoacid after optical excitation of the photoacid. $E°_{HB}$ and E^{*}_{HB} are the hydrogen-bond interaction energies in the ground and excited states, respectively. ν_{fl} and ν_a are the fluorescence and absorption transition frequencies. The arrows symbolize the pump–probe experiment.

One may also try to empirically correlate between the bond-length changes occurring at O–H···O coordinate and the increase in the acidity of photoacid upon electronic excitation. Such a study is currently in progress using a comparative examination of a large set of photoacids and utilizing bond-energy-bond order models.[47] Our preliminary study is in general agreement with the observations of Humphrey and Pratt[65–66] and Leutwyler and co-workers,[67–69] although it may overestimate the decrease in the O···O distance as a function of the increase in the acidity of the photoacid in the electronic excited state (Figure 18).

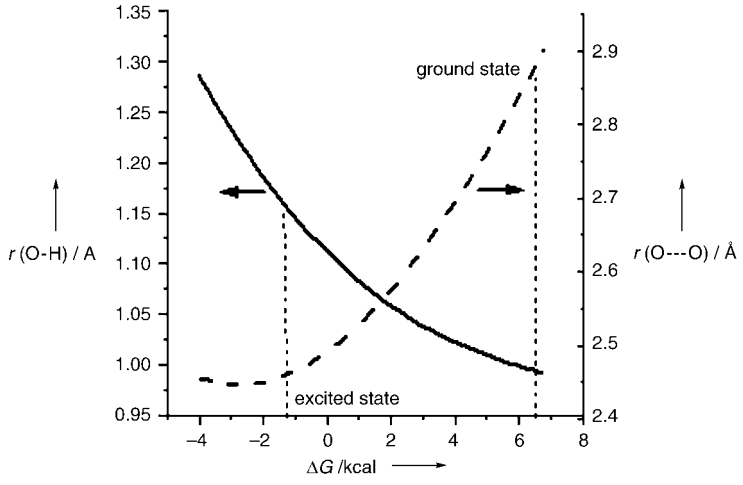

Figure 18. Correlation between the free energy of the proton transfer to water of phenol-like photoacids and the two bond lengths in the O–H···O coordinates using bond-energy-bond-order theory.[39] (——): O–H bond-length, (-----): O···O separation length. The crossing points of the dotted lines indicate the bond lengths in the ground and excited states of the photoacid using the known proton-dissociation free energies of the two states in water.

Finally, we address the possibility of intramolecular processes occurring in the excited photoacid and affecting its transient excited-state absorption dynamics on the sub-100 fs time scale. These include vibrational cooling, vibrational energy redistribution and singlet-singlet transitions. Our arguments against such phenomena significantly complicating the transient evolution of the excited-state absorption spectrum of the photoacid are based upon self-consistent arguments and the double control (pure solvents without a complexing base control and the methoxy derivative of HPTA in presence of a complexing base) that we have used in our measurements. The effect of hydrogen bonding on HPTA is clearly evident from the steady-state optical and IR spectra and is not observed in the control measurements in the pure solvents and on MPTA. According to the general view of the effect of hydrogen bonding on the optical spectra of a chromophore, the effect of the hydrogen-bonding interaction is additive to the effect of the nonspecific polar interactions of the solvent. This assumption forms the basis for the highly useful Kamlet–Taft analysis and for the establishment of various empirical solvent polarity scales. The validity of this empirical concept is nicely demonstrated in our own experiments where mixtures of very small amounts of DMSO in DCM and DCE exhibit almost the same effect on the absorption spectra of HPTA as the much more polar solvent DMSO. Moving to the time-resolved results, the presence of hydrogen-bonding agents have not only resulted in an additional sub-100 fs decay component, but also in the increase in the overall amplitude of the spectral shift, exactly as expected from the steady-state measurements. In comparison, no such behavior was observed in the time and energy evolution of the transient absorption in our two control measurements.

Yet another indication for the validity of the assignment of the sub-100 ps component in our experiments to hydrogen-bonding interaction may be found in preliminary femtosecond-time-resolved mid-IR studies which have been carried out recently by the Nibbering group. Within their time resolution (150 fs) and up to 1 ns, no significant time-evolution was found in the vibrational fingerprint region of the aromatic rings of HPTA (1250–1700 cm^{-1}) when it was dissolved in various solvents including DMSO and was optically excited at 400 nm, the same excitation wavelength used in our optical pump–probe measurements. In addition, there was little change between the vibronic patterns of HPTA in the strong hydrogen-bonding solvents DMSO and methanol (both deuterated) and in the much weaker hydrogen-bonding solvent of much less polarity, deuterated chloroform, indicating that HPTA is in a similar electronic state in all of the checked solvents regardless of the strength of the hydrogen-bonding interaction or of solvent polarity. Also, exciting the photoacid in DMSO with excess energy (calculated as the difference between the excitation energy at 400 nm and the position of the steady-state absorption maximum at 430 nm) of 1740 cm^{-1} has appeared to cause little extra vibrational activity. It is thus un-

likely that the excess 270 cm^{-1} of excitation energy over the one used in our control MPTA experiment is the reason for the additional ultrafast component observed in the transient absorption of the hydrogen-bonded HPTA. We conclude that the preliminary fs-resolved IR measurements done so far by the Nibbering group on HPTA do not support the existence of an intramolecular process in HPTA-base complexes which may be responsible for the acid-base hydrogen-bonding complex behaving profoundly differently from either the uncomplexed HPTA or its methoxy analogue.

7. Summary

Following the change in the potential energy surface of the HPTA molecule upon electronic excitation we propose some geometric changes in the pre-existing hydrogen-bonding complex between HPTA and various oxygen bases. It is likely that in response to the increased acidity of the photoacid in the electronic excited state, the equilibrium (average) bond length of the intermolecular hydrogen bond formed in the ground state by the acidic proton shortens and relaxes to a new geometry, a relaxation process which may involve the participation of several intermolecular vibrational modes including the stretch vibration of the hydrogen-bonding O···O atoms. Our fs-resolved transient-absorption measurements suggest that this relaxation process occurs within less than 100 fs, and perhaps as fast as within 50 fs, even faster than the inertial solvent response found in the polar dielectric solvation of the pure solvents. Our present resolution does not allow us to determine if this "in flight" relaxation of the hydrogen-bonding interaction is purely exponential. It is reasonable to assume that it is a distributed function influenced by both the excited- and ground-state distributions in the hydrogen-bond length and bending angles and by the temporal distribution in the phase of the hydrogen-bond stretch mode. It also remains to be seen if this movement is overdamped or shows some oscillatory motion as predicted theoretically for hydrogen-bond relaxation after vibrational hole-burning in pure water, as was recently verified experimentally by Fecko et al.[72]

Experimental Section

The femtosecond excitation source was a regenerative Ti:sapphire amplifier pumped optical parametric amplifier (OPA) system as described in details previously.[55] Briefly, a mode-locked femtosecond Ti:sapphire oscillator (Coherent, Mira Seed) was used to seed a Ti:-sapphire regenerative amplifier (Coherent, RegA 9050), which generates typically 50 fs (full width at the half maximum, FWHM) pulses at $\approx$800 nm with a repetition rate of 250 kHz. The output of this amplifier was split, and the major portion was frequency doubled using a 0.4 mm-thick crystal of beta-barium borate (BBO) in an OPA (Coherent, 9450) to produce pump pulses centered at 403 nm. A dual prism compressor consisting of two quartz prisms with a spacing of 110 cm was employed to compensate for the group velocity dispersion induced by the optics in the OPA and in the experimental setup. The pump pulse was directed to a stepping-motor-driven optical delay stage (MM3000, Newport) with 0.6 fs resolution prior to focusing on the sample. The minor part of the amplifier output (30%) was focused on a 2-mm thick sapphire plate to generate a white-light continuum as a probe pulse. The residual intense $\approx$800 nm light in the white-light continuum was removed using a short-pass cutoff filter (CVI, SPF-750–1.0) mounted in front of the sample. After passing thought the sample, the probing beam was directed into a monochromator (ISA) with a spectral resolution of 4 nm and the transmission changes induced by the pump pulse (ΔT) at selected wavelengths were monitored by a silicon photodiode (Thorlabs, PD210) connected to a lock-in amplifier with a spectral resolution of 4 nm. To obtain an absolute absorption change (ΔOD or $\Delta T/T$) at each probing wavelength, the transmission of the probe light (T) at the corresponding wavelength was measured separately by placing the chopper in the probing beam while the pump beam was blocked. A $\lambda/2$ plate was installed in the pump beam to set the polarization of the pump beam at the magic angle (54.7°) with respect to the probe beam. The typical pump pulse energy was kept at 8 nJ, and no observable difference was found for the kinetics measured under a ten-times lower pump intensity. The typical cross-correlation function between pump and probe pulses was 110–130 fs in duration depending on the probe wavelength, as judged by the profiles of the two-photon absorption signals of pure solvents, and the initial part of the kinetics recorded using stable laser dye solutions. A 1 mm thick quartz cell was used for the measurements and the typical sample OD was about 1.0 mm^{-1}. The sample cell was translated slowly within the focal plane of pump beam during the data acquisition whenever necessary. HPTA and methoxy-PTA, MPTA, [Figure 1(b)] were purchased from Fluka. All solvents were spectroscopic grade and anhydrous. To avoid a large concentration of DMSO, we have carried out our measurements in solutions where about 80% of the HPTA molecules were complexed with DMSO, which is about the optimal point in the concentration/complexation yield curve. The concentration of DMSO was 9×10^{-3} M. In the case of the less polar solvent dioxane, the concentration of the base was increased to 10^{-1} M. In all cases the complexation level of HPTA was judged by UV/Vis emission and absorption spectroscopy. All measurements were made at room temperature.

Acknowledgements

The authors wish to acknowledge B. Z. Magnes for carrying out the IR measurements shown in Figure 2. G.R.F. acknowledges financial support of the National Science Foundation. E.P. acknowledges the partial financial support of the James Franck Center for laser-matter interaction.

Keywords: femtochemistry · hydrogen-bonding interactions · photoacids · pump-probe spectroscopy · solvation dynamics

[1] M. Maroncelli, G. R. Fleming, *J. Chem. Phys.* **1987**, *86*, 6221.
[2] E. W. Castner Jr, M. Maroncelli, G. R. Fleming, *J. Chem. Phys.* **1987**, *86*, 1090.
[3] S. J. Rosenthal, X. Xie, M. Du, G. R. Fleming, *Chem. Phys.* **1991**, *95*, 4715.
[4] R. Jimenez, G. R. Fleming, P. V. Kumar, M. Maroncelli, *Nature* **1994**, *369*, 471.
[5] X. J. Jordanides, M. J. Lang, X. Song, G. R. Fleming, *J Phys. Chem. B* **1999**, *103*, 7995.
[6] C. F. Chapman, R. S. Fee, M. Maroncelli, *J. Phys. Chem.* **1995**, *99*, 4811.
[7] M. L. Horng, J. A. Gardecki, A. Papazyan, M. Maroncelli, *J. Phys. Chem.* **1995**, *99*, 17311.
[8] R. M. Stratt, M. Maroncelli, *J. Phys. Chem.* **1996**, *100*, 12981.
[9] J. D. Simon, *Acc. Chem. Res.* **1988**, *21*, 128.
[10] P. J. Rossky, J. D. Simon, *Nature* **1990**, *370*, 263.

[11] M. A. Kahlow, T. J. Kang, P. F. Barbara, *J. Chem. Phys.* **1998**, *88*, 2372.
[12] W. Jarzeba, G. C. Walker, A. E Johnson, P. F. Barbara, *Chem. Phys.* **1991**, *152*, 57.
[13] P. F. Barbara, W. Jarzeba, *Adv. Photochem.* **1990**, *15*, 1.
[14] Y. Jiang, P. K. McCarthy, G. J. Blanchard, *Chem. Phys.* **1994**, *183*, 249.
[15] S. A. Kovalenko, J. Ruthmann, N. P. Ernsting, *Chem. Phys. Lett.* **1997**, *271*, 40.
[16] J. Yu, M. J. Berg, *Chem. Phys.* **1992**, *96*, 8741.
[17] S. A. Kovalenko, J. Ruthmann, N. P. Ernsting, *J. Chem. Phys.* **1998**, *109*, 1894.
[18] J. Ruthmann, S. A. Kovalenko, N. P. Ernsting, D. J. Ouw, *J. Chem. Phys.* **1998**, *109*, 5466.
[19] E. T. J. Nibbering, K. Duppen, D. A. Wiersma, *J. Chem. Phys.* **1990**, *93*, 5477.
[20] E. T. J. Nibbering, K. Duppen, D. A. Wiersma, *J. Photochem. Phtobiol. A* **1992**, *62*, 347.
[21] W. P. de Boeij, M. S. Pshenichnikov, D. A. Wiersma, *Annu. Rev. Phys. Chem.* **1998**, *49*, 99.
[22] S. Yeremenko, M. S. Pshenichnikov, D. A. Wiersma, *Chem. Phys Lett.* **2003**, *369*, 107.
[23] J. Kim, U. W. Schmit, J. A. Gruetzmaher, G. A. Voth, N. E. Scherer, *J. Chem. Phys.* ***2002****, 116,* 737.
[24] T. Fonseca, B. M. Ladanyi, *J. Mol. Liq.* **1994**, *60*, 1.
[25] B. M. Ladani, R. M. Stratt, *J. Phys. Chem.* **1996**, *100*, 126.
[26] J. Feader, B. M. Ladanyi, *J. Phys. Chem. B* **2001**, *105*, 11148.
[27] C. Chudoba, E. T. J. Nibbering, T. Elsaesser, *Phys. Rev. Lett.* **1998**, *81*, 3010.
[28] C. Chudoba, E. T. J. Nibbering, T. Elsaesser, *J. Phys. Chem. A* **1999**, *103*, 5625.
[29] E. T. J. Nibbering, C. Chudoba, T. Elsaesser, *Isr. J. Chem.* **1999**, *39*, 333.
[30] E. T. J. Nibbering, T. Elsaesser, *Chem. Rev.* **2004**, *104*, 1887.
[31] F. Tschirschwitz, E. T. J. Nibbering, *Chem. Phys. Lett.* **1999**, *312*, 169.
[32] E. T. J. Nibbering, F. Tschirschwitz, C. Chudoba, T. Elsaesser, *J. Phys. Chem. A* **2000**, *104*, 4236.
[33] D. K. Palit, T. Zhang, S. Kumazaki, K. Yoshihara, *J. Am. Chem. Soc.* **2003**, *107*, 10789.
[34] R. W. Taft, J.-L. Abboud, M. J. Kamlet, *J. Am. Chem. Soc.* **1981**, *103*, 1080.
[35] M. H. Abraham, G. J. Buist, P. L. Grellier, R. A. McGill, D. V. Prior, S. Oliver, E. Turner, J. J. Morris, P. J. Taylor, P. Nicolet, P.-C. Maria, J.-F. Gal, J.-L. Abboud, R. M. Doherty, M. J. Kamlet, W. J. Shuely, R. W. Taft, *J. Phys. Org. Chem.* **1989**, *2*, 540.
[36] C. Reichardt, *Solvents and Solvent Effects in Organic Chemistry*, 2nd ed., VCH, Weinheim, **1990**.
[37] K. Ando, J. T. Hynes, *J. Mol. Liq.* **1995**, *64*, 25.
[38] G. A. Jeffrey, W. Saenger, *Hydrogen Bonding in Biological Structures*, Springer-Verlag, Berlin, **1991**.
[39] B.-Z. Magnes, D. Pines, N. Strashnikova, E. Pines, *Solid State Ionics* **2004**, *168*, 225.
[40] G. C. Pimentel, A. L. McClellan in *The Hydrogen Bond*, Freeman, San Francisco, **1960**, pp. 67 – 141.
[41] P. A. Kollman, L. C. Allen, *Chem. Rev.* **1972**, *72*, 3.
[42] M. D. Joesten, L. J. Schaad, *Hydrogen Bonding*, Marcel Dekker, New York, **1974**, pp. 2 – 27.
[43] G. Zundel in *The Hydrogen Bond—Recent Development in Theory and Experiments* (Eds.: P. Shuster, G Zundel, C. Sandorfy), North-Holland, Amsterdam, **1976**, pp. 683 – 766.
[44] M. Rozenberg, L. Schuss, Y. Marcus, *Phys. Chem. Chem. Phys.* **2000**, *2*, 2699.
[45] R. M. Badger, S. H. Bauer, *J. Am. Chem. Soc.* **1962**, *84*, 3817.
[46] K. F. Purcell, R. S. Drago, *J. Am. Chem. Soc.* **1967**, *89*, 2874.
[47] E. Pines in *Chemistry of Phenols*, (Ed.: Z. Rappoport), Wiley, **2003**, pp. 491 – 529.
[48] Y. Marcus, *Ion Solvation*, John Wiley & Sons Ltd., Chichester, **1985**, p. 186.
[49] L. M. Tolbert, J. E. Haubrich, *J. Am. Chem. Soc.* **1990**, *12*, 863.
[50] L. M. Tolbert, J. E. Haubrich, *J. Am. Chem. Soc.* **1994**, *116*, 10593.
[51] S. O. Shan, D. Hershlag, *Proc. Nat. Acad. Sci. USA* **1996**, *93*, 14474.
[52] E. M. Arnett, L. Joris, E. Mitchell, T. S. S. R. Murty, T. M. Gorrie, P. V. R. Schleyer, *Org. Biol. Chem.* **1972**, *92*, 2365.
[53] A. Tramer, M. Zaborowska, *Acta Phys. Pol.* **1968**, *34*, 821.
[54] D. Michael, I. Benjamin, *J. Chem. Phys.* **2001**, *114*, 2817.
[55] Q.-H. Xu, Y.-Z. Ma, G. R. Fleming, *Chem. Phys. Lett.* **2001**, *338*, 254.
[56] a) T.-H. Tran-Thi, T. Gustavsson, C. Prayer, S. Pommeret, J. T. Hynes, *Chem. Phys. Lett.* **2000**, 329, 421; b) J. T. Hynes, T.-H. Tran-Thi, T. Gustavsson, *J. Photochem. Photobiol. A* **2002**, *154*, 3; c) T.-H. Tran-Thi, C. Prayer, Ph. Millie, P. Uznanski, J. T. Hynes, *J. Phys. Chem.* A **2002**, *106*, 2244.
[57] *Ultrafast Hydrogen Bonding and Proton Transfer Processes in the Condensed Phase* (Eds.: T. Elsaesser, H. J. Bakker) Kluwer, Dordrecht, **2002**.
[58] A. Novak, *Struct. Bonding (Berlin)* **1974**, *18*, 177.
[59] W. Mikenda, *J. Mol. Struct.* **1986**, *147*, 1.
[60] D. Hadzi, S. Bratos, *Hydrogen Bond* **1976**, *2*, 565.
[61] T. Fiebig, M. Chachisvilis, M. Manger, A. H. Zewail, A. Douhal, L. Garsia-Ochoa, A. de La Hoz Ayuso, *J. Phys. Chem.* A **1999**, *103*, 7419.
[62] M. Bonn, M. J. P. Brugmans, A. W. Kleyn, R. A. van Santen, H. J. Bakker, *Phys. Rev. Lett.* **1996**, *76*, 2440.
[63] A. J. Lock, S. Woutersen, H. J. Bakker, *J. Phys Chem. A* **2001**, *105*, 1238.
[64] Y. Li, J. M. Farrar, *J. Chem. Phys.* **2004**, *120*, 199.
[65] S. J. Humphrey, D. W. Pratt, *Chem. Phys. Lett.* **1996**, *257*, 169.
[66] S. J. Humphrey, D. W. Pratt, *J. Chem. Phys.* **1996**, *104*, 8332.
[67] T. Burgi, T. Droz, S. Leutwyler, *Chem. Phys. Lett.* **1995**, *246*, 291.
[68] D. Henseler, C. Tanner, H.-M. Frey, S. Leutwyler, *J. Chem. Phys.* **2001**, *115*, 4055.
[69] C. Wickleder, D. Henseler, S. Leutwyler, *J. Chem. Phys.* **2002**, *116*, 1850.
[70] F. Lahmani, A. Zehnacker-Rentien, M. Broquier, *J. Photochem. Photobiol. B*, **2002**, *154*, 41.
[71] V. Guallar, V. S. Batista, W. H. Miller, *J. Chem. Phys.* **1999**, *110*, 9922.
[72] C. J. Fecko, J. D. Eaves, J. J. Loparo, A. Tokmakoff, P. L. Geissler, *Science* **2003**, *301*, 1698.
[73] A. J. Beningo, E. Ahmed, M. Berg, *J. Chem. Phys.* **1996**, *104*, 7382.
[74] M. Rini, B.-Z. Magnes, E. Pines, E. T. J. Nibbering, *Science*, **2003**, *301*, 349.
[75] R. Bauer, G. Zundel, *J. Phys. Chem.* A **2002**, *106*, 5.
[76] G. Zundel, *J. Mol. Struct.* **1996**, *381*, 23.
[77] R. Rey, K. B. Møller, J. T. Hynes, *J. Phys. Chem.* **2002**, *106*, 11993.
[78] K. B. Møller, R. Rey, J. T. Hynes *J. Phys Chem. A* **2004**, *108,* 1275.

Received: October 8, 2003
Revised: June 9, 2004

